

# A Search for Selectrons and Squarks at HERA

H1 Collaboration

## Abstract

Data from electron-proton collisions at a center-of-mass energy of 300 GeV are used for a search for selectrons and squarks within the framework of the minimal supersymmetric model. The decays of selectrons and squarks into the lightest supersymmetric particle lead to final states with an electron and hadrons accompanied by large missing energy and transverse momentum. No signal is found and new bounds on the existence of these particles are derived. At 95% confidence level the excluded region extends to 65 GeV for selectron and squark masses, and to 40 GeV for the mass of the lightest supersymmetric particle.

S. Aid<sup>14</sup>, V. Andreev<sup>26</sup>, B. Andrieu<sup>29</sup>, R.-D. Appuhn<sup>12</sup>, M. Arpagaus<sup>37</sup>, A. Babaev<sup>25</sup>, J. Bähr<sup>36</sup>, J. Bán<sup>18</sup>, Y. Ban<sup>28</sup>, P. Baranov<sup>26</sup>, E. Barrelet<sup>30</sup>, R. Barschke<sup>12</sup>, W. Bartel<sup>12</sup>, M. Barth<sup>5</sup>, U. Bassler<sup>30</sup>, H.P. Beck<sup>38</sup>, H.-J. Behrend<sup>12</sup>, A. Belousov<sup>26</sup>, Ch. Berger<sup>1</sup>, G. Bernardi<sup>30</sup>, R. Bernet<sup>37</sup>, G. Bertrand-Coremans<sup>5</sup>, M. Besançon<sup>10</sup>, R. Beyer<sup>12</sup>, P. Biddulph<sup>23</sup>, P. Bispham<sup>23</sup>, J.C. Bizot<sup>28</sup>, V. Blobel<sup>14</sup>, K. Borras<sup>9</sup>, F. Botterweck<sup>5</sup>, V. Boudry<sup>29</sup>, A. Braemer<sup>15</sup>, W. Braunschweig<sup>1</sup>, V. Brisson<sup>28</sup>, P. Bruel<sup>29</sup>, D. Bruncko<sup>18</sup>, C. Brune<sup>16</sup>, R. Buchholz<sup>12</sup>, L. Büngener<sup>14</sup>, J. Bürger<sup>12</sup>, F.W. Büsler<sup>14</sup>, A. Buniatian<sup>12,39</sup>, S. Burke<sup>19</sup>, M.J. Burton<sup>23</sup>, G. Buschhorn<sup>27</sup>, A.J. Campbell<sup>12</sup>, T. Carli<sup>27</sup>, M. Charlet<sup>12</sup>, D. Clarke<sup>6</sup>, A.B. Clegg<sup>19</sup>, B. Clerboux<sup>5</sup>, S. Cocks<sup>20</sup>, J.G. Contreras<sup>9</sup>, C. Cormack<sup>20</sup>, J.A. Coughlan<sup>6</sup>, A. Courau<sup>28</sup>, M.-C. Cousinou<sup>24</sup>, G. Cozzika<sup>10</sup>, L. Criegee<sup>12</sup>, D.G. Cussans<sup>6</sup>, J. Cvach<sup>31</sup>, S. Dagoret<sup>30</sup>, J.B. Dainton<sup>20</sup>, W.D. Dau<sup>17</sup>, K. Daum<sup>35</sup>, M. David<sup>10</sup>, C.L. Davis<sup>19</sup>, B. Delcourt<sup>28</sup>, A. De Roeck<sup>12</sup>, E.A. De Wolf<sup>5</sup>, M. Dirkmann<sup>9</sup>, P. Dixon<sup>19</sup>, P. Di Nezza<sup>33</sup>, W. Dlugosz<sup>8</sup>, C. Dollfus<sup>38</sup>, J.D. Dowell<sup>4</sup>, H.B. Dreis<sup>2</sup>, A. Droutskoi<sup>25</sup>, D. Düllmann<sup>14</sup>, O. Dünger<sup>14</sup>, H. Duhm<sup>13</sup>, J. Ebert<sup>35</sup>, T.R. Ebert<sup>20</sup>, G. Eckerlin<sup>12</sup>, V. Efremenko<sup>25</sup>, S. Egli<sup>38</sup>, R. Eichler<sup>37</sup>, F. Eisele<sup>15</sup>, E. Eisenhandler<sup>21</sup>, R.J. Ellison<sup>23</sup>, E. Elsen<sup>12</sup>, M. Erdmann<sup>15</sup>, W. Erdmann<sup>37</sup>, E. Evrard<sup>5</sup>, A.B. Fahr<sup>14</sup>, L. Favart<sup>28</sup>, A. Fedotov<sup>25</sup>, D. Feeken<sup>14</sup>, R. Felst<sup>12</sup>, J. Feltesse<sup>10</sup>, J. Ferencei<sup>18</sup>, F. Ferrarotto<sup>33</sup>, K. Flamm<sup>12</sup>, M. Fleischer<sup>9</sup>, M. Flieser<sup>27</sup>, G. Flügge<sup>2</sup>, A. Fomenko<sup>26</sup>, B. Fominykh<sup>25</sup>, J. Formánek<sup>32</sup>, J.M. Foster<sup>23</sup>, G. Franke<sup>12</sup>, E. Fretwurst<sup>13</sup>, E. Gabathuler<sup>20</sup>, K. Gabathuler<sup>34</sup>, F. Gaede<sup>27</sup>, J. Garvey<sup>4</sup>, J. Gayler<sup>12</sup>, M. Gebauer<sup>36</sup>, A. Gellrich<sup>12</sup>, H. Genzel<sup>1</sup>, R. Gerhards<sup>12</sup>, A. Glazov<sup>36</sup>, U. Goerlach<sup>12</sup>, L. Goerlich<sup>7</sup>, N. Gogitidze<sup>26</sup>, M. Goldberg<sup>30</sup>, D. Goldner<sup>9</sup>, K. Golec-Biernat<sup>7</sup>, B. Gonzalez-Pineiro<sup>30</sup>, I. Gorelov<sup>25</sup>, C. Grab<sup>37</sup>, H. Grässler<sup>2</sup>, R. Grässler<sup>2</sup>, T. Greenshaw<sup>20</sup>, R.K. Griffiths<sup>21</sup>, G. Grindhammer<sup>27</sup>, A. Gruber<sup>27</sup>, C. Gruber<sup>17</sup>, J. Haack<sup>36</sup>, T. Hadig<sup>1</sup>, D. Haidt<sup>12</sup>, L. Hajduk<sup>7</sup>, M. Hampel<sup>1</sup>, W.J. Haynes<sup>6</sup>, G. Heinzelmann<sup>14</sup>, R.C.W. Henderson<sup>19</sup>, H. Henschel<sup>36</sup>, I. Herynek<sup>31</sup>, M.F. Hess<sup>27</sup>, W. Hildesheim<sup>12</sup>, K.H. Hiller<sup>36</sup>, C.D. Hilton<sup>23</sup>, J. Hladký<sup>31</sup>, K.C. Hoeger<sup>23</sup>, M. Höppner<sup>9</sup>, D. Hoffmann<sup>12</sup>, T. Holtom<sup>20</sup>, R. Horisberger<sup>34</sup>, V.L. Hudgson<sup>4</sup>, M. Hütte<sup>9</sup>, H. Hufnagel<sup>15</sup>, M. Ibbotson<sup>23</sup>, H. Itterbeck<sup>1</sup>, A. Jacholkowska<sup>28</sup>, C. Jacobsson<sup>22</sup>, M. Jaffre<sup>28</sup>, J. Janoth<sup>16</sup>, T. Jansen<sup>12</sup>, L. Jönsson<sup>22</sup>, K. Johannsen<sup>14</sup>, D.P. Johnson<sup>5</sup>, L. Johnson<sup>19</sup>, H. Jung<sup>10</sup>, P.I.P. Kalmus<sup>21</sup>, M. Kander<sup>12</sup>, D. Kant<sup>21</sup>, R. Kaschowitz<sup>2</sup>, U. Kathage<sup>17</sup>, J. Katzy<sup>15</sup>, H.H. Kaufmann<sup>36</sup>, O. Kaufmann<sup>15</sup>, S. Kazarian<sup>12</sup>, I.R. Kenyon<sup>4</sup>, S. Kermiche<sup>24</sup>, C. Keuker<sup>1</sup>, C. Kiesling<sup>27</sup>, M. Klein<sup>36</sup>, C. Kleinwort<sup>12</sup>, G. Knies<sup>12</sup>, T. Köhler<sup>1</sup>, J.H. Köhne<sup>27</sup>, H. Kolanoski<sup>3</sup>, F. Kole<sup>8</sup>, S.D. Kolya<sup>23</sup>, V. Korbel<sup>12</sup>, M. Korn<sup>9</sup>, P. Kostka<sup>36</sup>, S.K. Kotelnikov<sup>26</sup>, T. Krämerkämper<sup>9</sup>, M.W. Krasny<sup>7,30</sup>, H. Krehbiel<sup>12</sup>, D. Krücker<sup>2</sup>, U. Krüger<sup>12</sup>, U. Krüner-Marquis<sup>12</sup>, H. Küster<sup>22</sup>, M. Kuhlen<sup>27</sup>, T. Kurča<sup>36</sup>, J. Kurzhöfer<sup>9</sup>, D. Lacour<sup>30</sup>, B. Laforge<sup>10</sup>, R. Lander<sup>8</sup>, M.P.J. Landon<sup>21</sup>, W. Lange<sup>36</sup>, U. Langenegger<sup>37</sup>, J.-F. Laporte<sup>10</sup>, A. Lebedev<sup>26</sup>, F. Lehner<sup>12</sup>, C. Leverenz<sup>12</sup>, S. Levonian<sup>29</sup>, Ch. Ley<sup>2</sup>, G. Lindström<sup>13</sup>, M. Lindstroem<sup>22</sup>, J. Link<sup>8</sup>, F. Linsel<sup>12</sup>, J. Lipinski<sup>14</sup>, B. List<sup>12</sup>, G. Lobo<sup>28</sup>, H. Lohmander<sup>22</sup>, J.W. Lomas<sup>23</sup>, G.C. Lopez<sup>13</sup>, V. Lubimov<sup>25</sup>, D. Lüke<sup>9,12</sup>, N. Magnussen<sup>35</sup>, E. Malinowski<sup>26</sup>, S. Mani<sup>8</sup>, R. Maraček<sup>18</sup>, P. Marage<sup>5</sup>, J. Marks<sup>24</sup>, R. Marshall<sup>23</sup>, J. Martens<sup>35</sup>, G. Martin<sup>14</sup>, R. Martin<sup>20</sup>, H.-U. Martyn<sup>1</sup>, J. Martyniak<sup>7</sup>, T. Mavroidis<sup>21</sup>, S.J. Maxfield<sup>20</sup>, S.J. McMahon<sup>20</sup>, A. Mehta<sup>6</sup>, K. Meier<sup>16</sup>, T. Merz<sup>36</sup>, A. Meyer<sup>12</sup>, A. Meyer<sup>14</sup>, H. Meyer<sup>35</sup>, J. Meyer<sup>12</sup>, P.-O. Meyer<sup>2</sup>, A. Migliori<sup>29</sup>, S. Mikocki<sup>7</sup>, D. Milstead<sup>20</sup>, J. Moeck<sup>27</sup>, F. Moreau<sup>29</sup>, J.V. Morris<sup>6</sup>, E. Mroczko<sup>7</sup>, D. Müller<sup>38</sup>, G. Müller<sup>12</sup>, K. Müller<sup>12</sup>, P. Murín<sup>18</sup>, V. Nagovizin<sup>25</sup>, R. Nahnauer<sup>36</sup>, B. Naroska<sup>14</sup>, Th. Naumann<sup>36</sup>, P.R. Newman<sup>4</sup>, D. Newton<sup>19</sup>, D. Neyret<sup>30</sup>, H.K. Nguyen<sup>30</sup>, T.C. Nicholls<sup>4</sup>, F. Niebergall<sup>14</sup>, C. Niebuhr<sup>12</sup>, Ch. Niedzballa<sup>1</sup>, H. Niggli<sup>37</sup>, R. Nisius<sup>1</sup>, G. Nowak<sup>7</sup>, G.W. Noyes<sup>6</sup>, M. Nyberg-Werther<sup>22</sup>, M. Oakden<sup>20</sup>, H. Oberlack<sup>27</sup>, U. Obrock<sup>9</sup>, J.E. Olsson<sup>12</sup>, D. Ozerov<sup>25</sup>, P. Palmen<sup>2</sup>, E. Panaro<sup>12</sup>, A. Panitch<sup>5</sup>, C. Pascaud<sup>28</sup>, G.D. Patel<sup>20</sup>, H. Pawletta<sup>2</sup>, E. Peppel<sup>36</sup>, E. Perez<sup>10</sup>, J.P. Phillips<sup>20</sup>, A. Pieuchot<sup>24</sup>, D. Pitzl<sup>37</sup>, G. Pope<sup>8</sup>, S. Prell<sup>12</sup>, R. Prosi<sup>12</sup>, K. Rabbertz<sup>1</sup>, G. Rädcl<sup>12</sup>, F. Raupach<sup>1</sup>, P. Reimer<sup>31</sup>, S. Reinshagen<sup>12</sup>, H. Rick<sup>9</sup>, V. Riech<sup>13</sup>, J. Riedlberger<sup>37</sup>, F. Riepenhausen<sup>2</sup>, S. Riess<sup>14</sup>, E. Rizvi<sup>21</sup>, S.M. Robertson<sup>4</sup>,

P. Robmann<sup>38</sup>, H.E. Roloff<sup>36,†</sup>, R. Roosen<sup>5</sup>, K. Rosenbauer<sup>1</sup>, A. Rostovtsev<sup>25</sup>, F. Rouse<sup>8</sup>, C. Royon<sup>10</sup>, K. Rüter<sup>27</sup>, S. Rusakov<sup>26</sup>, K. Rybicki<sup>7</sup>, N. Sahlmann<sup>2</sup>, D.P.C. Sankey<sup>6</sup>, P. Schacht<sup>27</sup>, S. Scharein<sup>15</sup>, S. Schiek<sup>14</sup>, S. Schleich<sup>16</sup>, P. Schleper<sup>15</sup>, W. von Schlippe<sup>21</sup>, D. Schmidt<sup>35</sup>, G. Schmidt<sup>14</sup>, A. Schöning<sup>12</sup>, V. Schröder<sup>12</sup>, E. Schuhmann<sup>27</sup>, B. Schwab<sup>15</sup>, F. Sefkow<sup>38</sup>, M. Seidel<sup>13</sup>, R. Sell<sup>12</sup>, A. Semenov<sup>25</sup>, V. Shekelyan<sup>12</sup>, I. Sheviakov<sup>26</sup>, L.N. Shtarkov<sup>26</sup>, G. Siegmon<sup>17</sup>, U. Siewert<sup>17</sup>, Y. Sirois<sup>29</sup>, I.O. Skillicorn<sup>11</sup>, P. Smirnov<sup>26</sup>, J.R. Smith<sup>8</sup>, V. Solochenko<sup>25</sup>, Y. Soloviev<sup>26</sup>, A. Specka<sup>29</sup>, J. Spiekermann<sup>9</sup>, S. Spielman<sup>29</sup>, H. Spitzer<sup>14</sup>, F. Squinabol<sup>28</sup>, R. Starosta<sup>1</sup>, M. Steenbock<sup>14</sup>, P. Steffen<sup>12</sup>, R. Steinberg<sup>2</sup>, H. Steiner<sup>12,40</sup>, B. Stella<sup>33</sup>, A. Stellberger<sup>16</sup>, J. Stier<sup>12</sup>, J. Stiewe<sup>16</sup>, U. Stöblein<sup>36</sup>, K. Stolze<sup>36</sup>, U. Straumann<sup>15</sup>, W. Struczinski<sup>2</sup>, J.P. Sutton<sup>4</sup>, S. Tapprogge<sup>16</sup>, M. Taševský<sup>32</sup>, V. Tchernyshov<sup>25</sup>, S. Tchetchelnitski<sup>25</sup>, J. Theissen<sup>2</sup>, C. Thiebaux<sup>29</sup>, G. Thompson<sup>21</sup>, P. Truöl<sup>38</sup>, J. Turnau<sup>7</sup>, J. Tutas<sup>15</sup>, P. Uelkes<sup>2</sup>, A. Usik<sup>26</sup>, S. Valkár<sup>32</sup>, A. Valkárová<sup>32</sup>, C. Vallée<sup>24</sup>, D. Vandenplas<sup>29</sup>, P. Van Esch<sup>5</sup>, P. Van Mechelen<sup>5</sup>, Y. Vazdik<sup>26</sup>, P. Verrecchia<sup>10</sup>, G. Villet<sup>10</sup>, K. Wacker<sup>9</sup>, A. Wagener<sup>2</sup>, M. Wagener<sup>34</sup>, A. Walther<sup>9</sup>, B. Waugh<sup>23</sup>, G. Weber<sup>14</sup>, M. Weber<sup>12</sup>, D. Wegener<sup>9</sup>, A. Wegner<sup>27</sup>, T. Wengler<sup>15</sup>, M. Werner<sup>15</sup>, L.R. West<sup>4</sup>, T. Wilksen<sup>12</sup>, S. Willard<sup>8</sup>, M. Winde<sup>36</sup>, G.-G. Winter<sup>12</sup>, C. Wittek<sup>14</sup>, E. Wunsch<sup>12</sup>, J. Žáček<sup>32</sup>, D. Zarbock<sup>13</sup>, Z. Zhang<sup>28</sup>, A. Zhokin<sup>25</sup>, F. Zomer<sup>28</sup>, J. Zsembory<sup>10</sup>, K. Zuber<sup>16</sup>, and M. zurNedden<sup>38</sup>

<sup>1</sup> I. Physikalisches Institut der RWTH, Aachen, Germany<sup>a</sup>

<sup>2</sup> III. Physikalisches Institut der RWTH, Aachen, Germany<sup>a</sup>

<sup>3</sup> Institut für Physik, Humboldt-Universität, Berlin, Germany<sup>a</sup>

<sup>4</sup> School of Physics and Space Research, University of Birmingham, Birmingham, UK<sup>b</sup>

<sup>5</sup> Inter-University Institute for High Energies ULB-VUB, Brussels; Universitaire Instelling Antwerpen, Wilrijk; Belgium<sup>c</sup>

<sup>6</sup> Rutherford Appleton Laboratory, Chilton, Didcot, UK<sup>b</sup>

<sup>7</sup> Institute for Nuclear Physics, Cracow, Poland<sup>d</sup>

<sup>8</sup> Physics Department and IIRPA, University of California, Davis, California, USA<sup>e</sup>

<sup>9</sup> Institut für Physik, Universität Dortmund, Dortmund, Germany<sup>a</sup>

<sup>10</sup> CEA, DSM/DAPNIA, CE-Saclay, Gif-sur-Yvette, France

<sup>11</sup> Department of Physics and Astronomy, University of Glasgow, Glasgow, UK<sup>b</sup>

<sup>12</sup> DESY, Hamburg, Germany<sup>a</sup>

<sup>13</sup> I. Institut für Experimentalphysik, Universität Hamburg, Hamburg, Germany<sup>a</sup>

<sup>14</sup> II. Institut für Experimentalphysik, Universität Hamburg, Hamburg, Germany<sup>a</sup>

<sup>15</sup> Physikalisches Institut, Universität Heidelberg, Heidelberg, Germany<sup>a</sup>

<sup>16</sup> Institut für Hochenergiephysik, Universität Heidelberg, Heidelberg, Germany<sup>a</sup>

<sup>17</sup> Institut für Reine und Angewandte Kernphysik, Universität Kiel, Kiel, Germany<sup>a</sup>

<sup>18</sup> Institute of Experimental Physics, Slovak Academy of Sciences, Košice, Slovak Republic<sup>f</sup>

<sup>19</sup> School of Physics and Chemistry, University of Lancaster, Lancaster, UK<sup>b</sup>

<sup>20</sup> Department of Physics, University of Liverpool, Liverpool, UK<sup>b</sup>

<sup>21</sup> Queen Mary and Westfield College, London, UK<sup>b</sup>

<sup>22</sup> Physics Department, University of Lund, Lund, Sweden<sup>g</sup>

<sup>23</sup> Physics Department, University of Manchester, Manchester, UK<sup>b</sup>

<sup>24</sup> CPPM, Université d'Aix-Marseille II, IN2P3-CNRS, Marseille, France

<sup>25</sup> Institute for Theoretical and Experimental Physics, Moscow, Russia

<sup>26</sup> Lebedev Physical Institute, Moscow, Russia<sup>f</sup>

<sup>27</sup> Max-Planck-Institut für Physik, München, Germany<sup>a</sup>

<sup>28</sup> LAL, Université de Paris-Sud, IN2P3-CNRS, Orsay, France

<sup>29</sup> LPNHE, Ecole Polytechnique, IN2P3-CNRS, Palaiseau, France

<sup>30</sup> LPNHE, Universités Paris VI and VII, IN2P3-CNRS, Paris, France

<sup>31</sup> Institute of Physics, Czech Academy of Sciences, Praha, Czech Republic<sup>f,h</sup>

<sup>32</sup> Nuclear Center, Charles University, Praha, Czech Republic<sup>f,h</sup>

<sup>33</sup> INFN Roma and Dipartimento di Fisica, Università "La Sapienza", Roma, Italy

<sup>34</sup> Paul Scherrer Institut, Villigen, Switzerland

<sup>35</sup> Fachbereich Physik, Bergische Universität Gesamthochschule Wuppertal, Wuppertal, Germany<sup>a</sup>

<sup>36</sup> DESY, Institut für Hochenergiephysik, Zeuthen, Germany<sup>a</sup>

<sup>37</sup> Institut für Teilchenphysik, ETH, Zürich, Switzerland<sup>i</sup>

<sup>38</sup> Physik-Institut der Universität Zürich, Zürich, Switzerland<sup>i</sup>

<sup>39</sup> Visitor from Yerevan Phys. Inst., Armenia

<sup>40</sup> On leave from LBL, Berkeley, USA

† Deceased

<sup>a</sup> Supported by the Bundesministerium für Bildung, Wissenschaft, Forschung und Technologie, FRG, under contract numbers 6AC17P, 6AC47P, 6DO57L, 6HH17P, 6HH27L, 6HD17L, 6HD27L, 6KI17P, 6MP17L, and 6WT87P

<sup>b</sup> Supported by the UK Particle Physics and Astronomy Research Council, and formerly by the UK Science and Engineering Research Council

<sup>c</sup> Supported by FNRS-NFWO, IISN-IIKW

<sup>d</sup> Supported by the Polish State Committee for Scientific Research, grant nos. 115/E-743/SPUB/P03/109/95 and 2 P03B 244 08p01, and Stiftung für Deutsch-Polnische Zusammenarbeit, project no.506/92

<sup>e</sup> Supported in part by USDOE grant DE F603 91ER40674

<sup>f</sup> Supported by the Deutsche Forschungsgemeinschaft

<sup>g</sup> Supported by the Swedish Natural Science Research Council

<sup>h</sup> Supported by GA ČR, grant no. 202/93/2423, GA AV ČR, grant no. 19095 and GA UK, grant no. 342

<sup>i</sup> Supported by the Swiss National Science Foundation

# 1 Introduction

Supersymmetry [1] is presently considered to be a promising candidate for a theory beyond the Standard Model (SM) of particle physics. In particular the Minimal Supersymmetric extension of the Standard Model (MSSM) describes as well as the SM all experimental data, and in addition it offers solutions for some of the questions left open by the SM, such as the Higgs mass or the hierarchy problem. However, no direct evidence for supersymmetry has yet been found.

Supersymmetry relates fermions to bosons and predicts for each SM particle a partner with spin differing by half a unit. So sneutrinos and selectrons,  $(\tilde{\nu}_{eL}, \tilde{e}_L)$ ,  $\tilde{e}_R$ , are scalar partners of neutrinos and electrons,  $(\nu_{eL}, e_L)$ ,  $e_R$ , and similarly squarks  $(\tilde{u}_L, \tilde{d}_L)$ ,  $\tilde{u}_R, \tilde{d}_R$  are the partners of up and down quarks. Two Higgs doublets with vacuum expectation values  $v_2, v_1$  are necessary to give masses to up-type quarks ( $v_2$ ) and to down-type quarks and charged leptons ( $v_1$ ). The partners of the gauge bosons  $W^\pm, Z^0, \gamma$  and the two Higgs doublets are called gauginos and higgsinos. They can mix and form two charged mass eigenstates  $\chi_{1,2}^\pm$  (charginos) and four neutral mass eigenstates  $\chi_{1,2,3,4}^0$  (neutralinos).

Experimentally supersymmetric particles are constrained to be heavier than their SM partners and so supersymmetry must be broken. In the MSSM this leads to extra mass parameters  $M_2$  and  $M_1$  for the  $SU_2$  and  $U_1$  gauginos. Thus the masses of charginos and neutralinos depend on  $M_1, M_2, \tan\beta \equiv v_2/v_1$  and the higgsino mass parameter  $\mu$ . The gaugino–sfermion couplings are the same as in the SM, but via mixing the chargino and neutralino–sfermion couplings also depend on these supersymmetric parameters.

In the MSSM it is assumed that the multiplicative quantum number  $R$ -parity is conserved, where  $R_P = 1$  for the SM particles and  $R_P = -1$  for their superpartners. This implies that supersymmetric particles can only be produced in pairs and that the lightest of them, which generally is assumed to be the  $\chi_1^0$ , is stable. Since the  $\chi_1^0$  is neutral and only weakly interacting it will escape direct experimental detection.

At HERA the dominant MSSM process is the production of a selectron and a squark via neutralino exchange  $ep \rightarrow \tilde{e} \tilde{q} X$  as shown in Fig. 1. The  $\tilde{e}$  and  $\tilde{q}$  decay into any lighter gaugino and their SM partners. The decay involving  $\chi_1^0$  gives an experimentally clean signature of an electron, hadrons and missing energy and momentum. This is the channel analyzed here, where the proper branching ratios for  $\tilde{e} \rightarrow e\chi_1^0$  and  $\tilde{q} \rightarrow q\chi_1^0$  are taken into account.

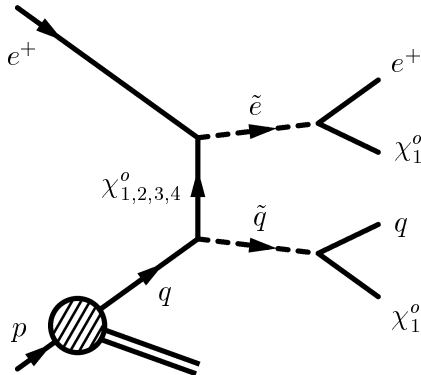


**Figure 1:** Feynman diagram for selectron - squark production via neutralino exchange and the subsequent decays into the lightest supersymmetric particle  $\chi_1^0$ .

In this paper it is assumed that the masses of  $\tilde{e}_L$  and  $\tilde{e}_R$  are identical. The same holds for the  $\tilde{q}$  states and mass degeneracy is also assumed for the superpartners of the four lightest

quarks. In order to reduce the number of free MSSM parameters it is assumed that  $M_1$  and  $M_2$  are related via the weak mixing angle  $\theta_W$ ,  $M_1 = 5/3 M_2 \tan^2 \theta_W$ , as suggested by Grand Unified Theories (GUT's) [1]. No other GUT relations are used. The parameter set given above specifies completely all couplings and masses involved.

At  $e^+e^-$  experiments masses below 45 GeV for selectrons and for squarks have been excluded by direct searches [2] and no attempt was made here to evaluate this excluded region. A search for selectron production at 130 and 136 GeV [3, 4] yielded a lower limit of  $M_{\tilde{e}} = 56$  GeV for  $M_{\chi_1^0} < 35$  GeV, but however, with different assumptions for the  $\tilde{e}_R, \tilde{e}_L$  mass splitting.

At the  $Z^0$  resonance direct searches for charginos and neutralinos [5] restrict the MSSM parameter space mainly for higgsino-like  $\chi_1^0$  and for  $\chi_1^0$  masses up to 20 GeV. These results are independent of  $M_{\tilde{e}}$  and  $M_{\tilde{\nu}}$ . Above the  $Z^0$  resonance recent searches have extended these limits considerably [3, 6, 4]. Here also  $\tilde{e}$  and  $\tilde{\nu}$  exchange contributes and, due to destructive interference, the constraints are most stringent for large  $M_{\tilde{e}}$  and  $M_{\tilde{\nu}}$ .

The experiments at the Tevatron  $p\bar{p}$  collider have obtained strong bounds on  $\tilde{q}$  masses. These limits however either depend on the assumption of a light  $\chi_1^0$  [7] or they are only valid for small gluino masses [8]. The latter bounds can only be related to the results obtained here if one assumes additional GUT relations between the gluino mass and  $M_2, M_1$ .

While this search deals with supersymmetric models with conserved  $R_P$ , the production of  $\tilde{q}$  in models with broken  $R_P$  has been considered in [9].

## 2 Detector description

A detailed description of the H1 apparatus can be found elsewhere [10]. The following briefly describes the components of the detector relevant to this analysis, which makes use mainly of the calorimeters.

The liquid Argon (LAr) calorimeter [11] extends with full azimuthal coverage over the polar angular range  $4^\circ < \theta < 153^\circ$ , where  $\theta$  is defined with respect to the proton beam direction ( $+z$  axis). The calorimeter is highly segmented and consists of an electromagnetic section with lead absorbers, corresponding to a depth of between 20 and 30 radiation lengths, and a hadronic section with steel absorbers. The total depth of the LAr calorimeter varies between 4.5 and 8 hadronic interaction lengths. Single particles are measured in the LAr calorimeter with energy resolutions of  $\sigma(E)/E \approx 0.11/\sqrt{E/\text{GeV}} \oplus 0.01$  for electrons and  $\sigma(E)/E \approx 0.5/\sqrt{E/\text{GeV}} \oplus 0.02$  for charged pions. The electromagnetic and hadronic energy scales are known to 2% and 5% respectively.

The calorimeter is surrounded by a superconducting solenoid providing a uniform magnetic field of 1.15 T parallel to the beam axis in the tracking region. A large instrumented iron structure surrounds the solenoid to serve as a return yoke for the magnetic flux and as an additional calorimeter of 4.5 hadronic interaction lengths to absorb tails of hadronic showers.

The backward region of the detector ( $151^\circ < \theta < 177^\circ$ ) was covered in 1994 by an electromagnetic lead-scintillator calorimeter, which was replaced in 1995 by a new lead-scintillating fibre calorimeter [12] with improved containment and angular coverage. A plug calorimeter covers the angular region  $0.75^\circ < \theta < 3.5^\circ$  around the forward beam pipe.

Charged particle tracks are measured in two concentric jet drift chambers and a forward tracking detector covering the polar angular range  $7^\circ < \theta < 165^\circ$ . In this analysis the tracking detectors are used for the determination of the event vertex only.

### 3 Data selection and analysis

The event sample corresponds to an integrated luminosity of  $6.38 \pm 0.13 \text{ pb}^{-1}$  and was collected by the H1 experiment in 1994 and 1995 during collisions of 27.5 GeV positrons<sup>1</sup> with 820 GeV protons.

First some event quantities which are used in the analysis are introduced. The quantity  $E - P_z$  is defined as  $\sum_i E_i(1 - \cos \theta_i)$  where the sum runs over all LAr and instrumented iron calorimeter energy deposits. The backward and plug calorimeters are used only as a veto. The (2 dimensional) transverse momentum vector of a single energy deposition is  $\vec{P}_{t,i} = E_i \sin \theta_i (\cos \phi_i, \sin \phi_i)$  with polar angle  $\theta_i$  and azimuthal angle  $\phi_i$ . The total transverse momentum vector  $\vec{P}_t$  is the vector sum of all  $\vec{P}_{t,i}$  in the LAr and iron calorimeter. The variable  $P_{t\parallel}$  ( $P_{t\perp}$ ) is defined as the absolute value of the component of  $\vec{P}_t$  which is parallel (perpendicular) to the transverse component of the identified scattered electron.

The following selection criteria are used:

1. Events must be accepted by a LAr calorimeter trigger for electrons which requires a local energy deposit of more than 8 GeV in a small region of the electromagnetic LAr calorimeter.
2. A vertex has to be found from measured charged tracks to be within 35 cm of the nominal interaction point.
3. An electron must be identified by its shower shape in the LAr calorimeter, it must have an energy greater than 10 GeV, and its transverse momentum has to exceed 8 GeV. The polar angle  $\theta_e$  must be in the range  $10^\circ < \theta_e < 135^\circ$  and the electron must be isolated in a cone of pseudorapidity and azimuthal angle of radius 0.5.
4. The energy deposited in the backward calorimeter has to be below 5 GeV.
5. The transverse momentum measured in the plug calorimeter must be below 2 GeV.
6. Filters against cosmic and beam halo muons are applied.
7. The quantity  $E - P_z$  must be below 40 GeV.
8. Either
  - (a) the polar angle of the “current quark” must fulfill  $\theta_q > 5^\circ$ . Assuming standard deep inelastic scattering kinematics,  $\theta_q$  can be calculated in the quark parton model from the scattered electron and the electron beam energy. To compensate for an undetected radiative photon in the initial state, the electron beam energy is reduced by the energy of this photon which is determined using the measured total  $E - P_z$ .
  - (b)  $P_{t\perp} > 3 \text{ GeV}$  and
  - (c)  $P_{t\parallel} > 2.5 \text{ GeV} + (E - P_z)/2$
 or
  - (d)  $P_{t\perp} > 7 \text{ GeV}$  and
  - (e)  $P_{t\parallel} > 3 \text{ GeV}$

The asymmetry of the HERA beam energies leads to a boost in the proton beam direction of the produced heavy  $\tilde{e}$  and  $\tilde{q}$  and their decay products. Therefore, in contrast to the majority of SM events, no energy deposition is expected in the backward region of the detector (cuts 3 and 4). Energy losses in the forward beam pipe can create large values of  $P_t$ . Such events are vetoed by cut 5.

---

<sup>1</sup>In this paper the generic name “electron” is used also for positrons.

Because of momentum conservation, the value  $E - P_z = 2 \times 27.5 \text{ GeV} = 55 \text{ GeV}$  of the initial state beam particles is expected also for the measured final state of most SM processes. Supersymmetric events would have a much smaller value of  $E - P_z$  due to the undetected  $\chi_1^0$ 's. This is demonstrated by the dashed histogram in Fig. 2a which shows a superposition of several hundred simulated  $\tilde{e} \tilde{q}$  events with  $M_{\tilde{e}} = M_{\tilde{q}} = 65 \text{ GeV}$  and various values of  $M_{\chi_1^0}$ .

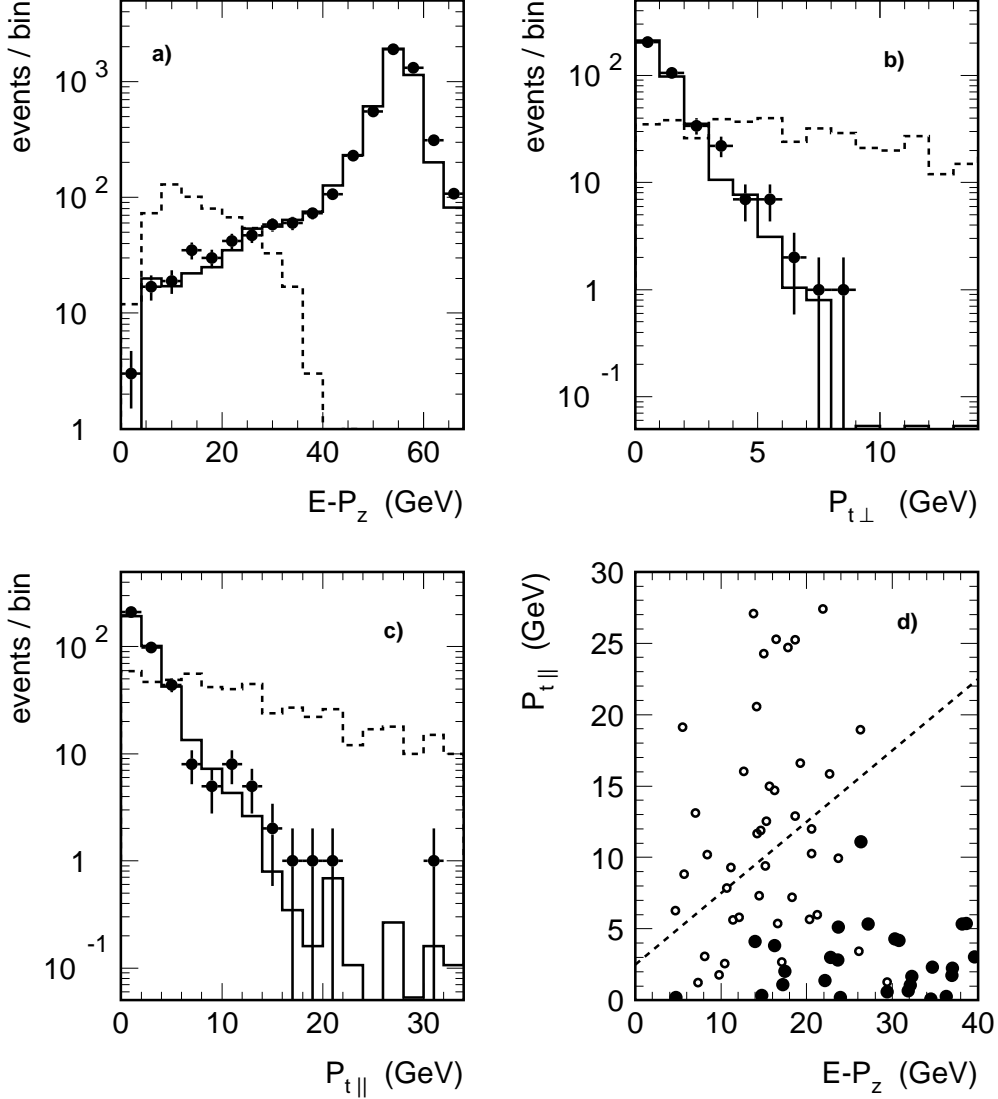


**Figure 2:** Comparison of data (points) with the expectation for all contributing SM processes (solid histogram). To indicate the signal region, simulated  $\tilde{e} \tilde{q}$  events are shown with arbitrary normalization by the dashed histogram for  $M_{\tilde{e}} = M_{\tilde{q}} = 65 \text{ GeV}$  and  $M_{\chi_1^0}$  between 35 and 55 GeV. Figure a) shows the  $E - P_z$  distribution after basic electron selection cuts 1–6. Figures b) and c) show the  $P_t$  component perpendicular ( $P_{t\perp}$ ) and parallel ( $P_{t\parallel}$ ) to the electron direction after applying an additional cut of  $E - P_z < 40 \text{ GeV}$ . Figure d) shows data (solid dots) and simulated  $\tilde{e} \tilde{q}$  events (open circles) after applying cuts 1–7, 8a and 8b (see text). The combined cut on  $P_{t\parallel} > 2.5 \text{ GeV} + (E - P_z)/2$  is indicated by the dashed line.

The event generator HERASUSY [13], which is used for this simulation, is based on the cross section for all four neutralino exchange diagrams and their interference [14]. All couplings and masses involved are determined using a modified version of the ISASUSY program [15]. The



PYTHIA program [16] is used for parton showers, string fragmentation and particle decays and a detailed simulation of the H1 detector response is included.

The events selected by cuts 1 – 6 are shown as solid points with statistical errors in Fig. 2a. They exhibit a clear peak at  $E - P_z = 55$  GeV and a long tail towards lower values. This distribution is well described by the solid histogram which represents a simulation of the contributing SM processes, i.e. neutral current and charged current deep inelastic scattering events simulated using the DJANGO program [17] and photoproduction events simulated using the PYTHIA program [16]. The tail towards low  $E - P_z$  is due to particles lost in the  $-z$  direction and is populated mainly by neutral current events with a photon radiated off the initial state electron. Contributing at very low  $E - P_z$  are also photoproduction processes, in which the scattered electron is not detected and a hard photon is misidentified as an electron in the event selection.

After cut 7 motivated by the HERASUSY simulation Fig. 2b and c show the distributions of  $P_{t\perp}$  and  $P_{t\parallel}$  for the remaining 384 events.  $367 \pm 19$  events are expected from all background sources. The resolution for  $P_{t\perp}$  is much better than for  $P_{t\parallel}$  since more energy is deposited collinear to the electron in SM processes. The extreme tails of the  $P_t$  distributions are populated by radiative charged current events with a photon misidentified as an electron. In all three distributions no obvious excess over expectation is observed.

Cut 8a on the jet angle predicted by the measured electron is employed in order to reduce the neutral current background of events with jets lost in the beam pipe. Also a minimum value of  $P_{t\perp}$  is required (cut 8b). Cut 8c on the correlation of  $P_{t\parallel}$  and  $E - P_z$  is illustrated in Fig. 2d which shows the data after cuts 1–7 and 8a together with a sample of simulated  $\tilde{e} \tilde{q}$  events. Cut 8c leads to a considerable loss for  $\tilde{e} \tilde{q}$  events with small values of  $P_{t\parallel}$ . A large fraction of these events are recovered by an alternative choice of cuts requesting mainly a large value of  $P_{t\perp}$  (cuts 8d and 8e).

After all cuts no events are found in a simulation of neutral current (photoproduction) processes in which there were 3 (0.63) times the statistics of the data. A background of  $0.6 \pm 0.2$  radiative charged current events is expected. No candidate event remains in the data.

## 4 Results

Having observed no signal, exclusion limits for  $\tilde{e} \tilde{q}$  production are derived.

The selection efficiency is determined using events generated as described above with the HERASUSY program for different values of  $M_{\tilde{e}}$ ,  $M_{\tilde{q}}$  and  $M_{\chi_1^0}$ . Other MSSM parameters do not influence the final state kinematics significantly. In order to interpolate between the simulated values for  $M_{\tilde{e}}$ ,  $M_{\tilde{q}}$  and  $M_{\chi_1^0}$  an empirical function  $\epsilon(\mathcal{P})$  is fitted to the simulated efficiency values. Here  $\mathcal{P}$  is defined via

$$\mathcal{P}^2 \equiv \frac{M_{\tilde{e}}^2 - M_{\chi_1^0}^2}{2 M_{\tilde{e}}} \times \frac{M_{\tilde{q}}^2 - M_{\chi_1^0}^2}{2 M_{\tilde{q}}}.$$

It characterizes the transverse momenta of electron and quark after the 2-body decays  $\tilde{e} \rightarrow e\chi_1^0$  and  $\tilde{q} \rightarrow q\chi_1^0$ . The efficiency  $\epsilon(\mathcal{P})$  reaches a plateau of 56% for  $\mathcal{P} > 25$  GeV. For smaller values of  $\mathcal{P}$  any signal in the detector becomes less and less significant and the efficiency drops to 50%, 18% and 0% for values of  $\mathcal{P} = 20, 10$  and 5 GeV respectively.

Systematic errors of this analysis originate in the efficiency parameterization, the electromagnetic and hadronic calorimeter energy scales, the parton density functions and the integrated

luminosity. The total systematic uncertainty amounts to 4.3% in the number of expected supersymmetric events.

In order to determine excluded regions in the MSSM parameter space, a systematic scan is performed for values of  $M_{\tilde{e}} \geq 45$  GeV,  $M_{\tilde{q}} \geq 45$  GeV,  $-1$  TeV  $\leq \mu \leq 1$  TeV,  $M_2 \geq 0$  GeV and  $1 \leq \tan\beta \leq 50$ . For each chosen set of these parameters the cross section, branching ratios and efficiency are evaluated yielding an expectation for the number of observed signal events. A parameter set is excluded when this number exceeds the 95% confidence level upper limit for 0 observed events taking into account the 4.3% systematic uncertainty mentioned above. Details of this statistical procedure are described in [18]. The resulting excluded regions in the MSSM parameter space are presented in the planes

- $M_{\chi_1^0}$  versus  $(M_{\tilde{e}} + M_{\tilde{q}})/2$  for constant  $\mu$  and  $\tan\beta = 1.41$  (Fig. 3)
- $M_{\tilde{e}}$  versus  $M_{\tilde{q}}$  for constant  $M_2$ ,  $\mu$  and  $\tan\beta = 1.41$  (Fig. 4)
- $M_2$  versus  $\mu$  for constant  $(M_{\tilde{e}} + M_{\tilde{q}})/2$  and  $\tan\beta = 1.41$  (Fig. 5)
- $M_2$  versus  $\tan\beta$  for constant  $(M_{\tilde{e}} + M_{\tilde{q}})/2$  and  $\mu$  (Fig. 6)

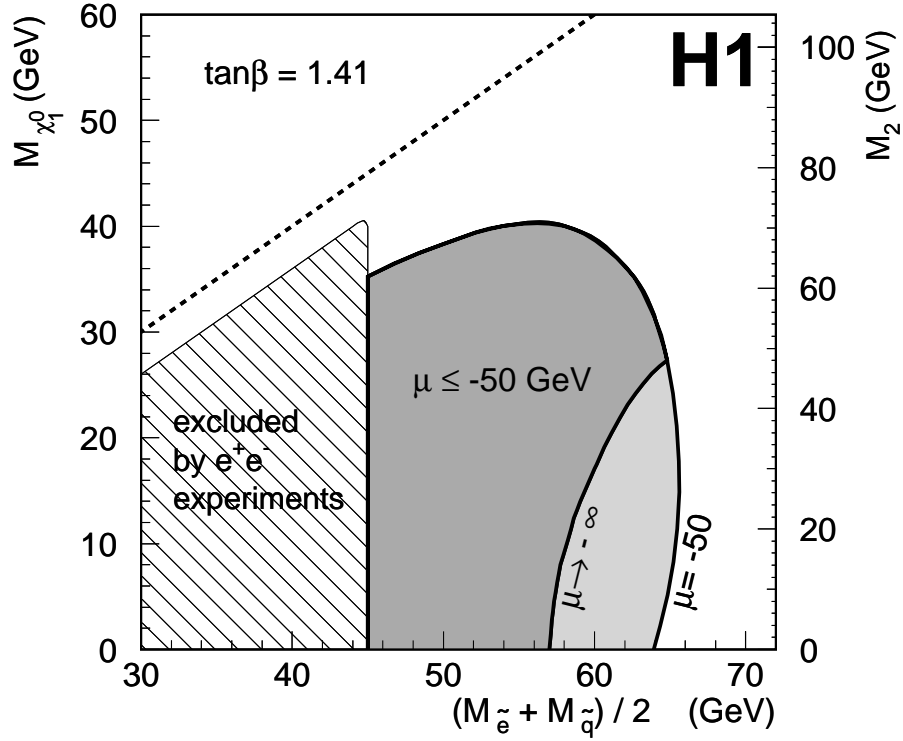
The choice of  $\tan\beta = 1.41$  is taken as typical of a low value for  $\tan\beta$ , and allows direct comparison with recent results obtained at LEP. The dependence on  $\tan\beta$  is shown in Fig. 6.

The cross section for  $\tilde{e} \tilde{q}$  production depends to first approximation on the  $\chi_1^0$  mass and couplings, and on the energy threshold for the hard process  $M_{\tilde{e}} + M_{\tilde{q}}$ . The neutralino and chargino masses scale roughly with  $M_2$  for  $\mu \ll 0$ . For the excluded parameter regions the branching ratios  $B(\tilde{e} \rightarrow \chi_1^0)$  and  $B(\tilde{q} \rightarrow \chi_1^0)$  are close to one because all other gauginos are heavier than  $M_{\tilde{e}}$  or  $M_{\tilde{q}}$ . Only at very small  $\mu$  and  $M_2$  other decays are possible, which have not been searched for in this paper.

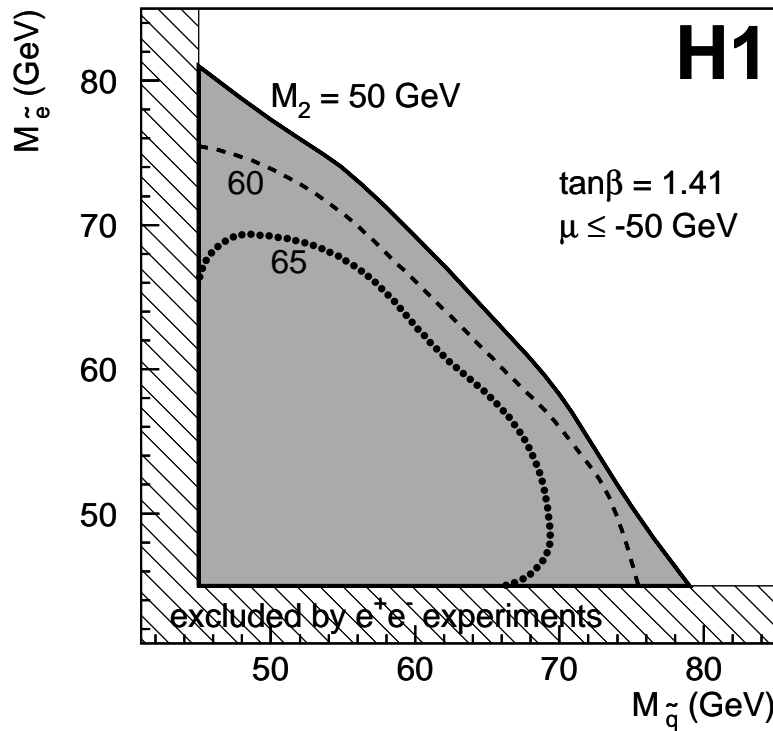
In Fig. 3 the plane  $M_{\chi_1^0}$  versus  $(M_{\tilde{e}} + M_{\tilde{q}})/2$  is shown for  $\tan\beta = 1.41$ . The dark and light shaded areas are excluded for  $\mu = -50$  GeV. For smaller values of  $\mu$  ( $\mu \rightarrow -\infty$ ) and for small  $M_2$  the competing decays into other gauginos lead to reduced limits for  $(M_{\tilde{e}} + M_{\tilde{q}})/2$ . The dark shaded area is excluded for all  $\mu \leq -50$  GeV. In the range  $\mu \leq -50$  GeV, and for this fixed value of  $\tan\beta$ , the  $\chi_1^0$  mass depends on  $M_2$  only, which is indicated by the second vertical scale on the right side of the figure. At large  $M_{\chi_1^0}$  the mass difference between  $\tilde{e}$ ,  $\tilde{q}$  and  $\chi_1^0$  becomes small and the efficiency drops correspondingly. Also the cross section is reduced due to the higher propagator mass. Both effects lead to reduced limits for  $(M_{\tilde{e}} + M_{\tilde{q}})/2$ . As seen from the distance between the shaded area and the diagonal line for  $M_{\chi_1^0} = M_{\tilde{e},\tilde{q}}$  this search is sensitive down to mass differences of  $\approx 10$  GeV. The excluded mass range extend to 65 GeV for  $(M_{\tilde{e}} + M_{\tilde{q}})/2$  and to 40 GeV for  $M_{\chi_1^0}$ . In particular the region  $(M_{\tilde{e}} + M_{\tilde{q}})/2 \leq 63$  GeV is excluded for  $M_{\chi_1^0} \leq 35$  GeV. Also shown are the limits obtained from direct searches for  $\tilde{e}$  and  $\tilde{q}$  pair production in  $Z^0$  decays [2].

Fig. 4 shows the excluded regions in  $M_{\tilde{e}}$  versus  $M_{\tilde{q}}$  for three different values of  $M_2$ . For a large range of  $M_{\tilde{e}}$  and  $M_{\tilde{q}}$  the limits are approximately a function of only the sum  $M_{\tilde{e}} + M_{\tilde{q}}$ , as used in Fig. 3. This approximation is valid for large mass differences between  $\tilde{e}$  and  $\chi_1^0$  and also between  $\tilde{q}$  and  $\chi_1^0$ , i.e.  $M_{\tilde{e},\tilde{q}} - M_{\chi_1^0} \geq 20$  GeV. The limits on  $M_{\tilde{e}}$  and  $M_{\tilde{q}}$  decrease when these differences become too small. For  $M_2 \approx 50$  GeV the highest mass bounds are reached, namely  $M_{\tilde{e}} = 77$  GeV at  $M_{\tilde{q}} = 50$  GeV and  $M_{\tilde{q}} = 75$  GeV at  $M_{\tilde{e}} = 50$  GeV.

In Fig. 5 the exclusion limits are shown in the  $M_2$  versus  $\mu$  plane for  $\tan\beta = 1.41$  and the mass ranges  $(M_{\tilde{e}} + M_{\tilde{q}})/2 \leq 60$  GeV and  $\leq 63$  GeV. For  $\mu \ll 0$  the  $\chi_1^0$  is dominated by its photino component. Consequently the coupling of  $\tilde{e}$  and  $\tilde{q}$  to the  $\chi_1^0$  are of electromagnetic strength and allow for a sizeable cross section. When  $\mu$  approaches 0 the  $\chi_1^0$  becomes higgsino-like and the



**Figure 3:** Excluded regions at 95% confidence level in the plane of  $M_{\chi_1^0}$  versus half the sum of  $M_{\tilde{e}}$  and  $M_{\tilde{q}}$  for  $\tan\beta = 1.41$ . The dark and light shaded areas are excluded for  $\mu = -50$  GeV. The dark shaded area is excluded for all  $\mu \leq -50$  GeV. The difference between both is due to decays into other gauginos than the  $\chi_1^0$ . The diagonal line corresponds to  $M_{\tilde{e},\tilde{q}} = M_{\chi_1^0}$ . The hatched area is excluded by direct searches for  $\tilde{e}$  and  $\tilde{q}$  pair production in  $Z^0$  decays [2]. The vertical axis is also labeled in terms of  $M_2$  (see text).



**Figure 4:** Exclusion limits at 95% confidence level in the  $M_{\tilde{e}}$  versus  $M_{\tilde{q}}$  plane for different values of  $M_2$  and  $\mu \leq -50$  GeV,  $\tan\beta = 1.41$ .  $M_{\tilde{e}}$  and  $M_{\tilde{q}}$  masses below 45 GeV are excluded by searches in  $Z^0$  decays. [2].

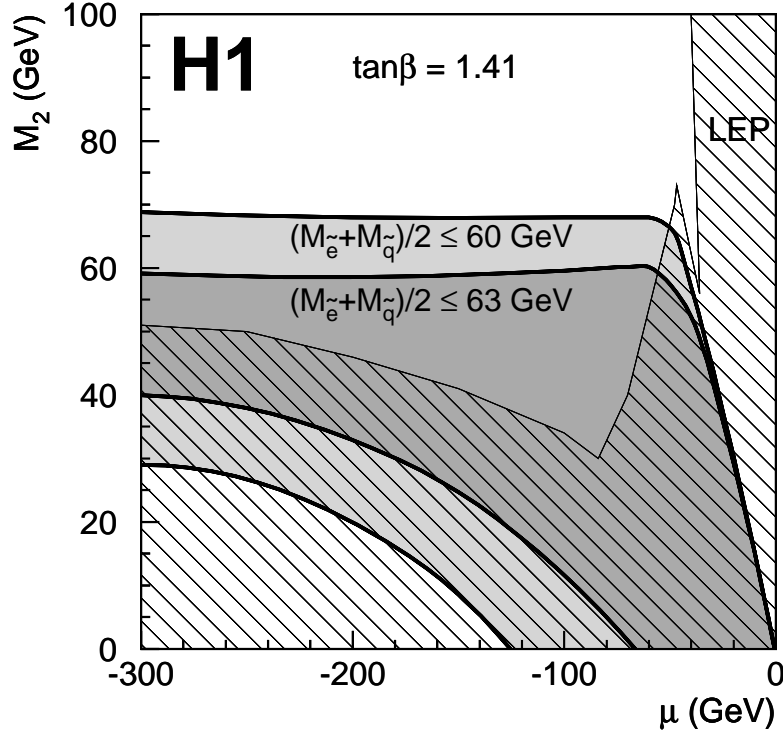


**Figure 5:** Domains excluded at 95% confidence level in the  $M_2$  versus  $\mu$  plane from the search for  $\tilde{e} \tilde{q}$  production for  $\tan\beta = 1.41$ . The dark shaded area corresponds to  $(M_{\tilde{e}} + M_{\tilde{q}})/2 \leq 63$  GeV, the additional light shaded area to  $(M_{\tilde{e}} + M_{\tilde{q}})/2 \leq 60$  GeV. The hatched areas show the most restrictive bounds obtained from  $e^+e^-$  collisions at LEP at center-of-mass energies around the  $Z^0$  mass and at 130 and 136 GeV [3], see text.

couplings and cross sections become very small. This defines the limit of the excluded parameter space for  $\mu$  close to 0. For  $\mu \ll 0$  the range excluded for  $M_2$  becomes independent of  $\mu$ . The region of  $\mu \ll 0$  and small  $M_2$  is not excluded because of decays into charginos and corresponds to the light shaded area in Fig. 3.

Also displayed as hatched areas in Fig. 5 are the most stringent bounds from searches for charginos and neutralinos at LEP at center-of-mass energies around the  $Z^0$  mass and at 130 and 136 GeV [3, 6]. These limits are valid for  $M_{\tilde{e},\tilde{\nu}} \geq 500$  GeV. For smaller masses the bounds are less restrictive. For  $\mu \ll 0$  the search presented here extends to considerably larger values for  $M_2$  than the LEP results. For  $\mu > 0$  however the LEP results are more restrictive. Therefore only values for  $\mu \leq 0$  are displayed.

In Fig. 6 the dependence of the  $M_2$  limits on  $\tan\beta$  is displayed for  $(M_{\tilde{e}} + M_{\tilde{q}})/2 \leq 60$  GeV and  $\mu = -200$  GeV. The limit on  $M_2$  rises to 80 GeV for large values of  $\tan\beta$ . The two symbols at  $\tan\beta = 1.41$  and 35 indicated the bounds from LEP as discussed above [3]. The range of  $M_2$  excluded in addition to those of LEP is largest for small values of  $\tan\beta$ .

## 5 Conclusion

Within the MSSM with conserved  $R$ -parity we have searched for  $\tilde{e} \tilde{q}$  pairs and their dominant decay modes into the lightest supersymmetric particle  $\chi_1^0$ . No signal was found and rejection

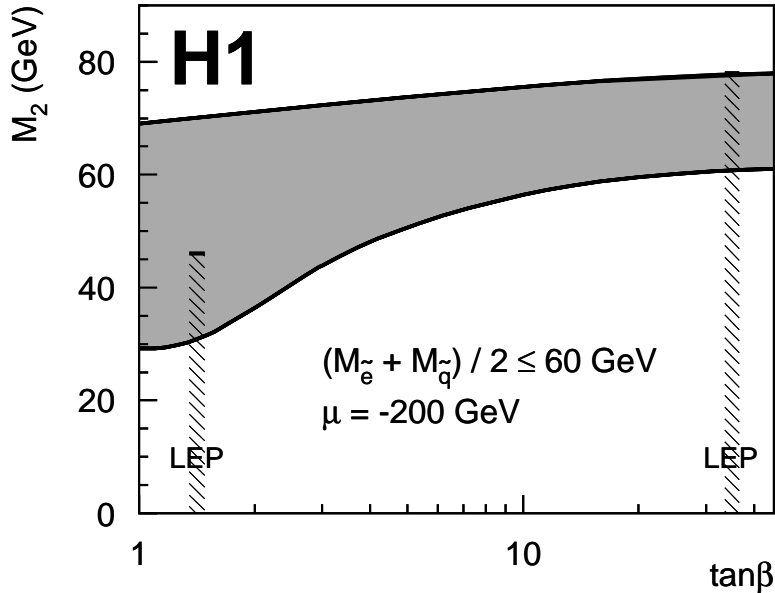


**Figure 6:** Excluded region at 95% confidence level for  $M_2$  as a function of  $\tan\beta$  for  $(M_{\tilde{e}} + M_{\tilde{q}})/2 \leq 60$  GeV and  $\mu = -200$  GeV (shaded area). The two symbols show the upper limits on  $M_2$  obtained for  $\tan\beta = 1.41$  and 35 from  $e^+e^-$  collisions at LEP for center-of-mass energies of 130 and 136 GeV [3].

limits at 95% confidence level are derived for the parameters  $M_{\tilde{e}}$ ,  $M_{\tilde{q}}$ ,  $M_2$ ,  $\mu$  and  $\tan\beta$ . The cross section, the branching ratios and the efficiency depend mainly on the sum  $M_{\tilde{e}} + M_{\tilde{q}}$  and on the  $\chi_1^0$  mass and couplings to fermions. The search is therefore most sensitive for a  $\chi_1^0$  with a large photino or  $\tilde{Z}$  component. For  $\tan\beta = 1.41$  masses up to  $(M_{\tilde{e}} + M_{\tilde{q}})/2 = 65$  GeV and up to  $M_{\chi_1^0} = 40$  GeV are probed. The dependence on  $\tan\beta$  is weak and mass limits improve towards large  $\tan\beta$ . The parameter region

$$(M_{\tilde{e}} + M_{\tilde{q}})/2 \leq 63 \text{ GeV for } M_{\chi_1^0} \leq 35 \text{ GeV and } \mu = -50 \text{ GeV}$$

is excluded. This limit applies as long as  $M_{\tilde{e},\tilde{q}} - M_{\chi_1^0} \geq 20$  GeV and decreases slightly when this difference becomes smaller. The result becomes independent of  $\mu$  for  $\mu \leq -50$  GeV. At small values of  $M_2$  the sensitivity is reduced due to decays into charginos.

For a photino-like  $\chi_1^0$  and small values of  $\tan\beta$  these results extend considerably the limits obtained by the searches for supersymmetry at LEP 1 and also those obtained while LEP was running at center of mass energies of 130 and 136 GeV. The limits, in particular for squarks, are independent of the gluino mass.

## Acknowledgments

We are grateful to the HERA machine group whose outstanding efforts made this experiment possible. We appreciate the immense effort of the engineers and technicians who constructed and maintained the detector. We thank the funding agencies for their financial support of the experiment. We wish to thank the DESY directorate for the support and hospitality extended to the non-DESY members of the collaboration.

## References

- [1] H.P.Nilles, Phys. Rep. **110** (1984) 1.  
H.Haber and G.Kane, Phys. Rep. **C117** (1985) 75.  
G.G.Ross, *Grand Unified Theories*, Benjamin Cummings (1985).  
For a recent review see  
H. Baer et. al., FSU-HEP-950401, hep-ph/953479 (1995), and references therein.
- [2] OPAL Collaboration, M.Z. Akrawy et al., Phys. Lett. **B240** (1990) 261.  
DELPHI Collaboration, P. Abreu et al., Phys. Lett. **B247** (1990) 148,  
ibid. **B247** (1990) 157.  
MARK II Collaboration, T. Barklow et al., Phys. Rev. Lett. **64** (1990) 2984.  
ALEPH Collaboration, D. Decamp et al., Phys. Rep. **216** (1992) 253.
- [3] ALEPH Collaboration, D. Buskulic et al., CERN preprint PPE-96-010 (1996).
- [4] L3 Collaboration, M. Acciarri et al., CERN preprint PPE-96-029 (1996).
- [5] L3 Collaboration, M. Acciarri et al., Phys. Lett. **B350** (1995) 109, and references therein.
- [6] OPAL Collaboration, G. Alexander et al., CERN preprint PPE-96-020 (1996).
- [7] CDF Collaboration, F. Abe et al., Phys. Rev. Lett. **69** (1992) 3439.
- [8] D0 Collaboration, S. Abachi et al., Phys. Rev. Lett. **75** (1995) 618.  
CDF Collaboration, F. Abe et al., Phys. Rev. Lett. **76** (1996) 2006.
- [9] H1 Collaboration, S. Aid et al., DESY preprint 96-056 (1996), accepted by Zeitschr. f. Physik and hep-ex/9604006.
- [10] H1 Collaboration, I. Abt et al., DESY internal report H1-96-01 (1996).  
H1 Collaboration, I. Abt et al., DESY preprint 93-103 (1993).
- [11] H1 Calorimeter Group, B. Andrieu et al., Nucl. Instr. and Meth. **A336** (1993) 460,  
ibid. **A336** (1993) 499, ibid. **A350** (1994) 57.
- [12] H1 SpaCal Group, T. Nicholls et al., DESY preprint 95-165 (1995) and DESY preprint 96-013 (1996).
- [13] P. Schleper, to be published in Proceedings of the workshop on Future Physics at HERA, DESY (1996).
- [14] J. Bartels and W. Hollik, Z. Phys. **C39** (1988) 433.
- [15] H. Baer, F. Paige, S. Protopopescu and X. Tata, Proceedings of the workshop on Physics at Current Accelerators and Supercolliders, ed. J. Hewett, A. White and D. Zeppenfeld, Argonne National Laboratory (1993).
- [16] T. Sjöstrand, Comp. Phys. Comm. **82** (1994) 74.
- [17] G. A. Schuler and H. Spiesberger, Proceedings of the workshop Physics at HERA, vol. 3, eds. W. Buchmüller, G. Ingelmann, DESY (1992) 1419.
- [18] H1 Collaboration, T. Ahmed et al., Z. Phys. **C64** (1994) 545.